Effective quasiparticle Hamiltonian based on Löwdin's orthogonalization

R. Sakuma,[1,2,3,*] T. Miyake,[2,3] and F. Aryasetiawan[1,2,3]
[1]*Graduate School of Advanced Integration Science, Chiba University, Chiba 263-8522, Japan*
[2]*Research Institute for Computational Sciences, National Institute of Advanced Industrial Science and Technology, Tsukuba, Ibaraki 305-8568, Japan*
[3]*Japan Science and Technology Agency, CREST, Kawaguchi, Saitama 332-0012, Japan*
(Received 28 August 2009; revised manuscript received 22 November 2009; published 18 December 2009)

Recently several schemes have been proposed to perform self-consistent GW calculations within a one-particle (quasiparticle) approximation. These so-called quasiparticle self-consistent GW schemes have been found to be successful in reproducing band gaps of semiconductors but there is some arbitrariness in the choice of the "effective" one-particle Hamiltonian in these schemes and their validity has not been assessed. To avoid ambiguity in choosing the one-particle Hamiltonian, we propose a scheme which is based on Löwdin's method of symmetric orthogonalization. In our approach we first calculate the true quasiparticle wave functions and energies with the real part of the frequency-dependent self-energy, and then orthonormalize these states using Löwdin's procedure to construct the effective quasiparticle Hamiltonian. Löwdin's procedure ensures that the obtained orthonormal orbitals are the closest to the original nonorthogonal quasiparticle wave functions in the least-square sense and uniquely defines the one-particle Hamiltonian. Unlike previous approaches, this approach takes into account the full frequency dependence and the off-diagonal elements of the self-energy without ambiguity. As test cases, we perform quasiparticle self-consistent GW calculations on NiO and Gd. We find that our results compare well with previous results obtained using a different effective Hamiltonian.

DOI: 10.1103/PhysRevB.80.235128 PACS number(s): 71.15.Qe, 71.20.−b, 71.27.+a

I. INTRODUCTION

The Green's function based approach within the GW approximation (GWA) (Ref. 1) has become the method of choice for calculating the quasiparticle band structures of materials since the pioneering work of Hybertsen and Louie[2,3] and Godby *et al.*[4] The GWA has since been applied to a wide range of systems[5,6] and recently the generalizations of the method to include higher-order correlation effects have been proposed.[7–10]

Despite its success, the GW method suffers from a serious problem associated with self-consistency. The fully self-consistent solution of Hedin's GW equations for the electron gas has been found to yield a larger occupied band width than the noninteracting value, in contradiction to the experimental results on the alkalis.[11] Results of self-consistent calculations in semiconductors seem to show too large band gaps although some controversies still remain.[12–14] In practice, the GW calculations are carried out in a nonself-consistent or "1-shot" way. The obvious problem of the 1-shot GW calculation is that the result inevitably depends on the initial states, which are in most cases taken to be the Kohn-Sham eigenstates of density-functional theory (DFT) within the local-density approximation (LDA). Several attempts have been reported to adopt better DFT approximations as a starting point[15–18] but it is difficult to improve the accuracy of the calculations in a systematic way.

As previously explained,[19–22] the failure of the (fully) self-consistent GWA is attributed to the "underscreening" effect originating from neglecting the vertex part. Due to the many-body effects the quasiparticle peaks of the Green's function are broadened and their weights are decreased, which leads to the underestimation of the polarization or the screening effect coming from the particle-hole excitation. A practical prescription to avoid this problem is to perform the calculation without the broadening effect, keeping the one-particle picture; that is, instead of solving the GW equations directly, one constructs from the GW self-energy some "effective" Hermitian potential or Hamiltonian and use the corresponding eigenstates to construct the GW self-energy for the next iteration. This cycle is repeated until convergence is reached.

The simplest self-consistent GW approach is "eigenvalue-only" or "diagonal-only" self-consistent GW scheme, in which the wave functions are fixed as the Kohn-Sham ones, and only the eigenenergies are calculated self-consistently. Since in many systems the Kohn-Sham eigenfunctions are found to be very close to the quasiparticle wave functions,[3] this is a reasonable approximation. However, in some materials the Kohn-Sham orbitals and energies do not form a good starting point and it is necessary to improve the wave functions. In such cases, the off-diagonal part of the self-energy cannot be neglected. In earlier work by Continenza *et al.*,[23] they approximated the self-energy by a static potential with a model dielectric function. In Ref. 24 the self-consistency in NiO was simulated by adding a static correction term on Ni e_g bands to the Kohn-Sham Hamiltonian. Of these schemes, one of the most successful is the quasiparticle self-consistent GW (QSGW) method proposed by Faleev *et al.*,[20–22] in which they proposed an effective one-body exchange-correlation potential that is constructed from the GW self-energy at some reference energies, whose form is formally derived by defining a measure of the difference between the self-energy and the effective potential and minimizing it. Recently Bruneval *et al.*[25] proposed to adopt the self-consistent static coulomb hole and screened exchange approximation to construct one-particle states, which are used in a subsequent 1-shot GW calculation.

Although these self-consistent GW schemes practically improve the quasiparticle spectra compared to the 1-shot GW results, especially for correlated materials such as transition-metal oxides, there is ambiguity in defining the static Hamiltonian since the self-energy is frequency dependent and not Hermitian. The objective of the present paper is to construct a unique effective Hamiltonian using Löwdin's method of symmetric orthogonalization.[26] By ensuring that the orthonormal eigenfunctions of the effective Hamiltonian are the closest to the nonorthogonal quasiparticle wave functions in the least-square sense, this procedure uniquely defines the one-particle Hamiltonian and takes into account the full frequency dependence and the off-diagonal elements of the self-energy without ambiguity. A precursor of the present scheme, which may be termed the quasiparticle mode (QPM) method,[27] was previously applied to the vanadium oxide in its simplified form and successfully reproduced the insulating phase. We then investigate how the different choices of the effective quasiparticle Hamiltonian affect the results. We first describe our scheme in detail and present results of the quasiparticle calculations of antiferromagnetic NiO and ferromagnetic Gd, whose quasiparticle energy levels are poorly reproduced by the LDA or the usual 1-shot GW scheme due to the presence of the localized d and f orbitals. We find that for these systems our scheme yields results which agree well with previous calculations based on the QSGW. Finally we discuss possible reasons and implications of our findings.

II. METHOD

In the GWA, the self-energy is approximated as[1,5]

$$\Sigma(\mathbf{r},\mathbf{r}',\omega) = \frac{i}{2\pi}\int G(\mathbf{r},\mathbf{r}',\omega+\omega')W(\mathbf{r},\mathbf{r}',\omega')d\omega'. \quad (1)$$

Here G is the one-particle Green's function and the screened coulomb interaction W is related to the polarization function P by $W=v+vPW$. In usual 1-shot GW calculations, G in Eq. (1) is replaced by a bare (noninteracting) Green's function calculated with Kohn-Sham eigenfunctions and energies $\{\psi^{KS}_{\mathbf{k}\mu}, \epsilon^{KS}_{\mathbf{k}\mu}\}$, and P is calculated within the random-phase approximation (RPA) as

$$P(\mathbf{r},\mathbf{r}',\omega) = \sum_{\text{spin}}\sum_{\mathbf{k}\mu}^{\text{occ}}\sum_{\mathbf{k}'\mu'}^{\text{unocc}} \psi^{*KS}_{\mathbf{k}\mu}(\mathbf{r})\psi^{KS}_{\mathbf{k}'\mu'}(\mathbf{r})\psi^{*KS}_{\mathbf{k}'\mu'}(\mathbf{r}')\psi^{KS}_{\mathbf{k}\mu}(\mathbf{r}') \times\left(\frac{1}{\omega+\epsilon^{KS}_{\mathbf{k}\mu}-\epsilon^{KS}_{\mathbf{k}'\mu'}+i\delta}-\frac{1}{\omega-\epsilon^{KS}_{\mathbf{k}\mu}+\epsilon^{KS}_{\mathbf{k}'\mu'}-i\delta}\right). \quad (2)$$

In the region where the imaginary part of the self-energy is small, the quasiparticle wave functions and energies are given as the solutions of

$$\det[\omega - h_0(\mathbf{k}) - \Re\Sigma(\mathbf{k},\omega)] = 0, \quad (3)$$

where h_0 is the Hartree Hamiltonian and $\Re$ denotes the Hermitian part. Due to the frequency dependence of Σ, the eigenvectors of Eq. (3) are, in general, not orthogonal.

The problem arises when one performs GW calculations self-consistently within a quasiparticle scheme, namely, how to construct orthonormal wave functions from the nonorthogonal quasiparticle states, or equivalently how to construct the effective one-particle Hamiltonian. The problem may be formulated as follows: given a set of linearly independent nonorthogonal quasiparticle wave functions $\{\Psi_{\mathbf{k}n}\}$ what would be the closest orthonormal orbitals $\{\psi_{\mathbf{k}\nu}\}$ to $\{\Psi_{\mathbf{k}\nu}\}$ in the least-square sense? Mathematically we wish to minimize

$$\Delta = \sum_{\mathbf{k}\nu}|\psi_{\mathbf{k}\nu}-\Psi_{\mathbf{k}\nu}|^2 \quad (4)$$

subject to the orthonormality of $\{\psi_{\mathbf{k}\nu}\}$. It has been proven by Carlson and Keller[28] that the set of orthonormal orbitals that fulfills this minimization condition can be constructed by using Löwdin's method of symmetric orthogonalization.[26] The set of orthonormal orbitals that minimizes Eq. (4) is given by

$$\psi = \Psi C, \quad CC^{+} = S^{-1}, \quad (5)$$

where

$$S_{\mu\nu} = \langle\Psi_{\mathbf{k}\mu}|\Psi_{\mathbf{k}\nu}\rangle \quad (6)$$

is the overlap matrix.

The Hermitian Hamiltonian that yields the closest orthonormal eigenfunctions to the given set of nonorthogonal quasiparticle states $\{E_{\mathbf{k}\nu}, \Psi_{\mathbf{k}\nu}\}$, in the least-square sense, is then given by

$$h^{\text{QPM}}(\mathbf{k}) = \sum_{\nu}|\psi_{\mathbf{k}\nu}\rangle E_{\mathbf{k}\nu}\langle\psi_{\mathbf{k}\nu}|. \quad (7)$$

It is worth noting that the eigenenergies of this Hamiltonian are the *same* as the quasiparticle energies obtained from the solutions of Eq. (3), as can be seen from Eq. (7). This form has an advantage in that there is no ambiguity arising from the frequency dependence of the self-energy and it works even in cases where the off-diagonal elements are large only for certain energy region so that it can be applied when the frequency dependence of the off-diagonal self-energy is important. We believe this approximation gives the closest states to the true quasiparticle states without ambiguity.

In our previous work,[27] which may be regarded as a precursor to Eq. (7) we proposed an effective quasiparticle Hamiltonian given by $h^{\text{QPM}}(\mathbf{k})=\Sigma_{\nu}|\Psi_{\mathbf{k}\nu}\rangle E_{\mathbf{k}\nu}\langle\Psi_{\mathbf{k}\nu}|$, where $\{E_{\mathbf{k}\nu}, \Psi_{\mathbf{k}\nu}\}$ are the eigenvalues and eigenvectors of Eq. (3). This form, however, has a potential problem due to a nonorthogonality of the quasiparticle wave functions; since $\Sigma_{\nu}|\Psi_{\mathbf{k}\nu}\rangle\langle\Psi_{\mathbf{k}\nu}|$ differs from unity, the eigenvectors of this Hamiltonian are not invariant with respect to a uniform shift of the energy level $E_{\mathbf{k}\nu}\rightarrow E_{\mathbf{k}\nu}+\lambda$.

Special care is needed in constructing the Hamiltonian by Eq. (7). Equation (3) can be solved iteratively or by a linearization[27] but, in general, the number of roots can be larger than the number of the one-particle states due to the dynamical correlation and those extra solutions appear in the spectra as satellite peaks. To adhere to the one-particle picture, the summation in Eq. (7) must be performed over only the quasiparticle solutions of Eq. (3); thus one has to pick out the quasiparticle solutions from all the solutions. In simple semiconductors it is easy to recognize plasmon satellites be-

cause the plasmon peak and quasiparticle peaks are well separated. However, in correlated systems the self-energy spectra becomes highly nonlinear and distinguishing the quasiparticle solutions and extra solutions can be difficult.

In this work, in each iteration we solve Eq. (3) by a linearization and when the number of roots in Eq. (3) is the same as the number of the bands considered, we use those solutions directly to construct the effective Hamiltonian h^{QPM}. When we find more solutions, we do not use the obtained states for calculating h^{QPM}; instead, we adopt the following first-order perturbation scheme to calculate the quasiparticle states, similar to the one in Ref. 29. After the ith iteration we have a set of (orthonormal) wave functions and energies $\{\psi^{(i)}_{\mathbf{k}\nu}, \epsilon^{(i)}_{\mathbf{k}\nu}\}$. From these states we calculate (nonorthogonal) quasiparticle wave functions according to $\Psi_{\mathbf{k}\nu} = \Sigma_\mu \alpha_{\mu\nu}(\mathbf{k})\psi^{(i)}_{\mathbf{k}\mu}$, where

$$\alpha_{\mu\nu}(\mathbf{k}) = \begin{cases} 1 & (\mu = \nu) \\ \dfrac{\langle \psi^{(i)}_{\mathbf{k}\mu} | \Re\Delta\Sigma(\epsilon^{(i)}_{\mathbf{k}\nu}) | \psi^{(i)}_{\mathbf{k}\nu} \rangle}{\epsilon^{(i)}_{\mathbf{k}\nu} - \epsilon^{(i)}_{\mathbf{k}\mu}} & (\mu \neq \nu) \end{cases} \tag{8}$$

and the quasiparticle energies are calculated as

$$E_{\mathbf{k}\nu} = \epsilon^{(i)}_{\mathbf{k}\nu} + Z\langle \psi^{(i)}_{\mathbf{k}\nu} | \Re\Delta\Sigma(\epsilon^{(i)}_{\mathbf{k}\nu}) | \psi^{(i)}_{\mathbf{k}\nu} \rangle. \tag{9}$$

Here $\Delta\Sigma$ is defined as $\Delta\Sigma = \Sigma + h_0 - h^{\mathrm{QPM}(old)}$, where $h^{\mathrm{QPM}(old)}$ is the QPM Hamiltonian [Eq. (7)] in a previous iteration used to construct $\{\psi^{(i)}_{\mathbf{k}\nu}, \epsilon^{(i)}_{\mathbf{k}\nu}\}$. The $(i+1)$th states $\{\psi^{(i+1)}_{\mathbf{k}\nu}, \epsilon^{(i+1)}_{\mathbf{k}\nu}\}$ are computed by diagonalizing Eq. (7) using the above $\{\Psi_{\mathbf{k}\nu}, E_{\mathbf{k}\nu}\}$. The change in the density in the Hartree potential is also taken into account. The renormalization factor Z in Eq. (9) can be calculated from the slope of $\langle \psi^{(i)}_{\mathbf{k}\nu} | \Re\Delta\Sigma(\omega) | \psi^{(i)}_{\mathbf{k}\nu} \rangle$ but in some cases due to the rapid variation in the self-energy with frequency the Z factor thus calculated can be too large or even negative. To avoid this instability, we fix Z for all the states. In this perturbation scheme the converged energies do not depend on the choice of Z because as one can see from Eq. (9) after the self-consistency is reached the second term of the right-hand side of Eq. (9) should be zero. To accelerate convergence, however, Z is set to 0.6. In the present calculations the extra solutions disappear after several iterations and the remaining solutions can be identified as the quasiparticle solutions.

In this paper, we compare the results of our scheme with those obtained with the diagonal-only self-consistent GW scheme and the QSGW scheme proposed by Faleev *et al.*;[20] in the latter the following form of the effective exchange-correlation potential is used:

$$\langle \psi_{\mathbf{k}\mu} | v^{\mathrm{eff}}_{xc} | \psi_{\mathbf{k}\nu} \rangle = \frac{1}{2}\Re[\Sigma_{\mu\nu}(\mathbf{k}, \epsilon_{\mathbf{k}\nu}) + \Sigma_{\mu\nu}(\mathbf{k}, \epsilon_{\mathbf{k}\mu})]. \tag{10}$$

The difference between their QSGW scheme and our scheme is that in the QSGW scheme it is the Hamiltonian, not the wave functions, that is optimized to simulate the quasiparticle states; in Ref. 22 the above effective potential is derived by minimizing the difference between the self-energy and the effective one-particle potential v^{eff}.

Our calculations are based on the full-potential linear-muffin-tin orbital (LMTO) code;[30] the details of the GW code is described in Ref. 22. Local orbitals corresponding to Ni 4*d* and Gd 5*f* states are included. In this work, the quasiparticle wave functions are always expanded in the LDA wave functions. The self-energy matrix is calculated by including 28 unoccupied bands for NiO and 21 (28) fully unoccupied bands for Gd majority-spin (minority-spin) channel, whose energies correspond to around 3 Ry above the Fermi energy. For other higher states we simulate the self-energy correction by shifting the LDA energy levels as is done in Ref. 22. We iterate until all the quasiparticle energies converge. In order to calculate the quasiparticle band structure near the Fermi energy, one has to calculate the self-energy and effective Hamiltonian at a very large number of k points along high-symmetry lines; instead of doing this cumbersome task we have used the band-structure interpolation scheme using the maximally localized Wannier function.[31,32] Similar interpolation scheme is recently reported in Ref. 33. We have used the program package WANNIER90.[34,35] We have used $4\times4\times4$ and $6\times6\times6$ k-point sampling for NiO and Gd, respectively. For simplicity we have assumed fcc lattice structure for Gd.

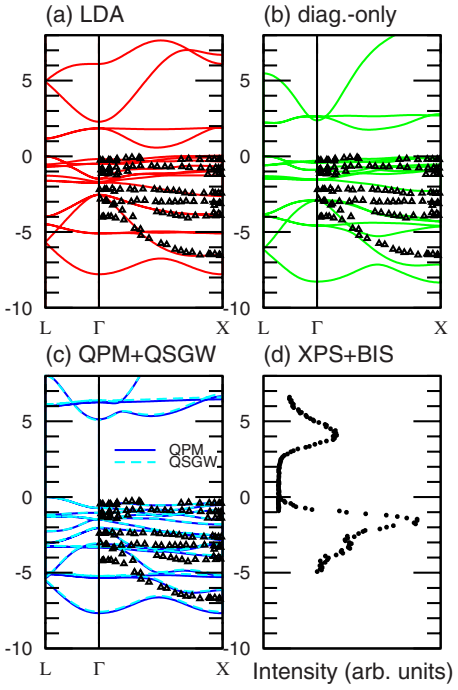

FIG. 1. (Color online) Band structure of antiferromagnetic NiO in eV calculated with (a) LDA, (b) diagonal-only self-consistent GW, and (c) QPM (solid lines) and QSGW (dashed lines). In each figure the ARPES data from Ref. 36 are also shown as triangles and the zero of the energy is set at the top of the valence band. (d) XPS and BIS spectra from Ref. 37.

III. RESULTS AND DISCUSSIONS

A. NiO

The band structures of antiferromagnetic NiO calculated with the (spin-dependent) LDA and self-consistent GW schemes are shown in Figs. 1(a)–1(c) and compared with available experimental angle-resolved photoemission spectroscopy (ARPES) data.[36] The x-ray photoelectron spectroscopy (XPS) and bremsstrahlung isochromat spectroscopy

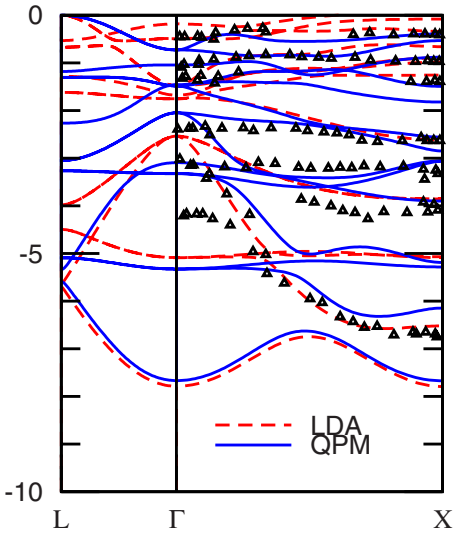

FIG. 2. (Color online) Comparison of the valence-band structure of antiferromagnetic NiO in eV calculated with LDA (dashed lines) and QPM (solid lines) together with the ARPES data from Ref. 36 (triangles). The zero of the energy is set at the top of the valence band.

(BIS) data[37] are also shown in Fig. 1(d). As is well known,[38] the LDA [Fig. 1(a)] yields a too small band gap compared to the experimental value of 4.2 eV. The lowest conduction band has mainly Ni minority-spin e_g character. The upper valence bands mostly consist of Ni $3d$ character and are separated from the lower valence bands with predominantly O $2p$ character. This is different from the commonly accepted charge-transfer interpretation of this material. In the diagonal-only self-consistent GW result [Fig. 1(b)], in agreement with previous work,[22] the e_g conduction band shifts upward by about 1 eV but the resulting band gap of ≈ 2 eV is still smaller than the experimental one. Furthermore, the dispersion of the occupied bands does not show any significant change; this result indicates the importance of the modification in the wave functions from the LDA ones, as previously reported.[24]

Our QPM result is shown in Fig. 1(c). In agreement with previous work,[22] our GW calculation yields a somewhat larger band gap of ≈ 5 eV than the experimental value of 4.2 eV. There are different views regarding the character of the lowest unoccupied state. One view interprets it to be of $4s$ character whereas another view interprets it to be of $3d$ character of e_{2g} symmetry. The GW calculation places the unoccupied $4s$ band lower than the narrow $3d$ band of e_{2g} symmetry but this may be due to a shortcoming of the self-consistent quasiparticle GW scheme which may tend to exaggerate the gap between the occupied t_{2g} band and the unoccupied e_g band. It has been systematically found in many cases that the quasiparticle self-consistent GW scheme often overestimates the band gaps. More accurate theory for systems with strong onsite correlations is clearly needed.

In Fig. 2 we compare the quasiparticle self-consistent GW result with the LDA result and ARPES data. The lowest band, as has been known for a long time, is not found experimentally. The broad oxygen $2p$ bands are relatively well reproduced already at the LDA level. Some deviations

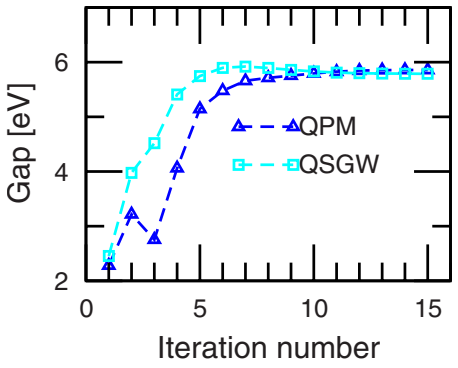

FIG. 3. (Color online) Direct band gap of NiO at $\mathbf{k}=(0,0,0)$ in each iteration within the QPM (triangles) and QSGW (squares). The lines are a guide to the eye.

around the Γ point are observed and the GW calculation does not seem to give much improvement, somewhat surprising considering that the GWA is expected to work well for describing extended states. Regarding the $3d$ bands, it is difficult to make a one-to-one comparison with experiment since the number of calculated bands considerably exceeds the number of experimentally observed bands. For the lower part of the $3d$ bands that hybridize with the oxygen $2p$ bands the GW result is in better agreement with experiment compared to the LDA result.

In Fig. 1(c) we compare also our result with the QSGW one. As can be seen, the two schemes give almost identical band structures, though we have used two different forms of the effective Hamiltonian and the two calculations follow different paths (see Fig. 3). We have found that in addition to the energy dispersion the calculated density distribution[39] and the self-energy spectra are very similar in these two methods; this means the two schemes reached the same fixed point. In order to confirm this, we construct the effective quasiparticle Hamiltonian in the QSGW scheme, $h^{\mathrm{QSGW}}=h_0+v_{xc}^{\mathrm{QSGW}}$, where v_{xc}^{QSGW} is given in Eq. (10), from the GW self-energy calculated with the effective quasiparticle wave functions and energies $\{\psi_{\mathbf{k}\nu},\epsilon_{\mathbf{k}\nu}\}$ obtained from the QPM scheme, and plot the off-diagonal elements of h^{QSGW} in Fig. 4. The result of the 1-shot GW calculation (i.e., $\{\psi_{\mathbf{k}\nu},\epsilon_{\mathbf{k}\nu}\}=\{\psi_{\mathbf{k}\nu}^{KS},\epsilon_{\mathbf{k}\nu}^{KS}\}$) is also shown for comparison. In the 1-shot GW result the off-diagonal elements are as large as ≈ 1 eV while

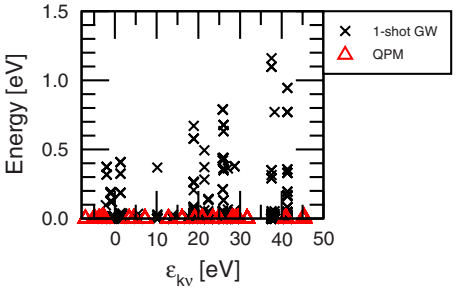

FIG. 4. (Color online) Matrix elements $|\langle\psi_{\mathbf{k}\mu}|h_0+v_{xc}^{\mathrm{QSGW}}|\psi_{\mathbf{k}\nu}\rangle|$ for $\mu<\nu$ at $\mathbf{k}=(0,0,0)$ as a function of $\epsilon_{\mathbf{k}\nu}$ within the 1-shot GW (crosses) and QPM (triangles). Here $v_{xc}^{\mathrm{QSGW}}=v_{xc}^{\mathrm{QSGW}}[\{\psi_{\mathbf{k}\nu},\epsilon_{\mathbf{k}\mu}\}]$ is calculated by using the wave functions and eigenenergies obtained in each scheme.

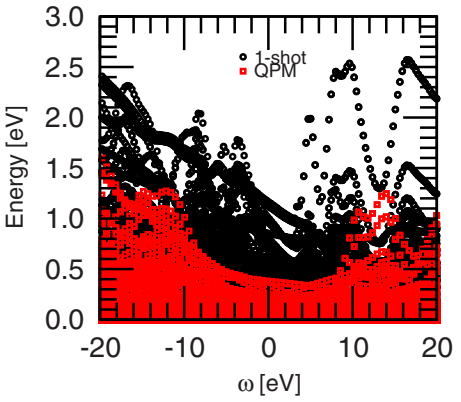

FIG. 5. (Color online) Off-diagonal elements of the Hartree Hamiltonian plus the self-energy of antiferromagnetic NiO $|\langle\psi_{\mathbf{k}\mu}|h_0(\mathbf{k})+\Re\Sigma(\mathbf{k},\omega)|\psi_{\mathbf{k}\mu}\rangle|$ in 1-shot GW (circles) and self-consistent QPM calculation (squares) for various bands at $\mathbf{k}=(0,0,0)$.

in the QPM result they are almost zero for all the bands considered, which means the states obtained in the self-consistent QPM calculation also diagonalize the QSGW Hamiltonian. This, however, does not mean that the off-diagonal self-energy completely disappears after self-consistency. In order to see this, in Fig. 5 we compare the off-diagonal elements of $|\langle\psi_{\mathbf{k}\mu}|h_0(\mathbf{k})+\Re\Sigma(\mathbf{k},\omega)|\psi_{\mathbf{k}\nu}\rangle|$ as a function of frequency for 1-shot GW and after the self-consistent QPM calculation. After self-consistency there still remain significant off-diagonal elements of $h_0+\Re\Sigma(\omega)$ of ≈ 1 eV that can be regarded as a measure of the difference between the "true" quasiparticle wave functions and "effective" ones that are subject to orthonormal condition. The self-consistent solution of the QPM or the QSGW calculations diagonalizes the particular form of the Hamiltonian h^{QSGW} but it is not the "eigenstates" of the quasiparticle equation [Eq. (3)].

In Fig. 5 it can be seen that while the 1-shot GW result shows a strong frequency dependence, after self-consistency is reached the off-diagonal self-energy becomes very smooth near the Fermi energy. This is a consequence of the large gap of ≈ 5 eV in the QPM result since in the RPA polarization [Eq. (2)] there is no transition less than the band gap and Im Σ becomes structureless in that energy region. This weak frequency dependence could be part of the reason why the QPM and QSGW yield the same results as in the latter the choice of the reference energy in Eq. (10) becomes irrelevant. However, considering that while the off-diagonal elements of $h_0+\Re\Sigma(\omega)$ is as large as ≈ 1 eV (Fig. 5) but those of h^{QSGW} (Fig. 4) are almost zero, this unexpected agreement is not explained by the structureless frequency spectra of the off-diagonal self-energy alone. We have indeed found that if we choose the effective potential as $\langle\psi_{\mathbf{k}\mu}|\tilde{v}_{xc}|\psi_{\mathbf{k}\nu}\rangle = \Re\Sigma_{\mu\nu}(\mathbf{k},\epsilon_{\mathbf{k}\nu})$ and calculate $\langle\psi_{\mathbf{k}\mu}|h_0+\tilde{v}_{xc}|\psi_{\mathbf{k}\nu}\rangle$ using the QPM wave functions and energies as is done to obtain Fig. 4, the off-diagonal elements of this Hamiltonian do not disappear, which indicates the frequency dependence of the self-energy cannot be simply neglected.

Self-consistency also changes the diagonal parts of the self-energy drastically; in Fig. 6 we plot the diagonal self-

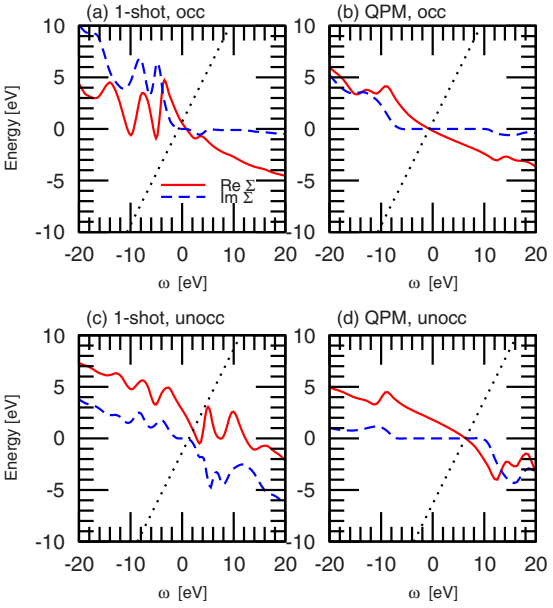

FIG. 6. (Color online) [(a) and (b)] Diagonal self-energy of the highest valence band and [(c) and (d)] the unoccupied e_g band of NiO at $\mathbf{k}=(0,0,0)$, obtained with [(a) and (c)] 1-shot GW and [(b) and (d)] QPM. Solid lines: $\mathrm{Re}\langle\psi_{\mathbf{k}\nu}|\Delta\Sigma(\mathbf{k},\omega)|\psi_{\mathbf{k}\nu}\rangle$. Dashed lines: $\mathrm{Im}\langle\psi_{\mathbf{k}\nu}|\Delta\Sigma(\mathbf{k},\omega)|\psi_{\mathbf{k}\nu}\rangle$. Dotted lines: $\omega-\epsilon_{\mathbf{k}\nu}$.

energy of the highest valence band [(a) and (b)] and the unoccupied Ni e_g band [(c) and (d)] in the 1-shot GW and self-consistent QPM calculation. A flat region appears in the imaginary part of Σ in the QPM results. Furthermore, while the 1-shot results are strongly frequency-dependent and LDA states are strongly renormalized with the renormalization factor $Z=0.5$, after self-consistency Z becomes rather large (≈ 0.8). The reason for these is again due to the increase in the band gap. Since the imaginary part of the self-energy is zero within the gap, through the Hilbert transform or the Kramers-Kronig relation the increase in the gap smoothes out the real part of the self-energy and at the same time reduces its slope over the gap resulting in larger Z factor. Physically, the increase in the band gap reduces the probability of the quasiparticle to decay by creating electron-hole excitations.

B. Gd

Ferromagnetic Gd is a "half-filled" system, where majority-spin f bands are fully occupied and minority-spin f bands are unoccupied. The experimental XPS and BIS data are available in Ref. 40 which is reproduced in Fig. 7(g); the position of occupied (unoccupied) f states is determined to be 7.44 (4.04)eV below (above) the Fermi level. In Figs. 7(a)–7(f) the calculated band structures of ferromagnetic Gd are shown. The LDA [Fig. 7(a) and 7(b)] fails to describe the correct f level of this system; the majority-spin f levels are located ≈ -5 eV below the Fermi level that are too shallow compared to experiment and the minority-spin f bands are located just above the Fermi level. The LDA is also known to fail to predict the ferromagnetic ground state[41] while the LDA+U scheme[42] correctly reproduces the ferromagnetic

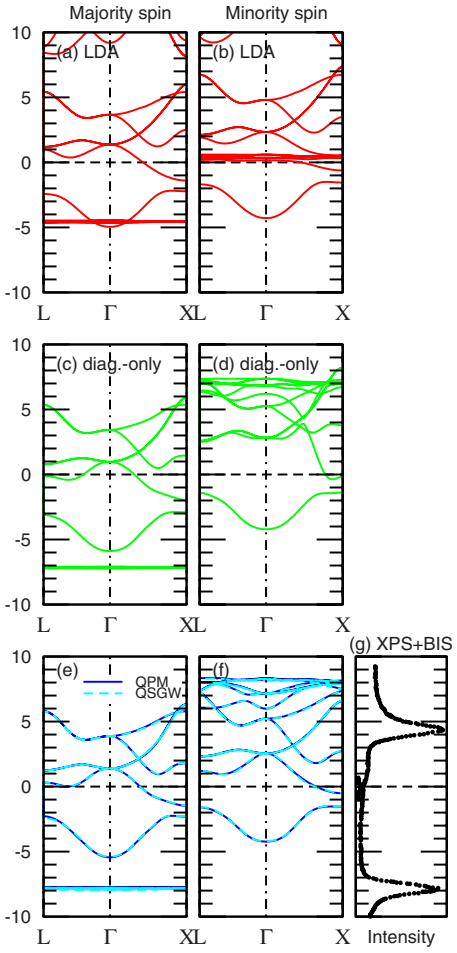

FIG. 7. (Color online) Band structure of Gd in eV calculated with [(a) and (b)] LDA, [(c) and (d)] diagonal-only self-consistent GW, [(e) and (f)] QPM (solid lines) and QSGW (dashed lines). Figures (a), (c), and (e) are of majority spin and (b), (d), and (f) are of minority spin. (g) XPS and BIS spectra of Gd from Ref. 40.

ground state and the positions of f levels.[43] In the diagonal-only self-consistent GW results [Figs. 7(c) and 7(d)] the majority-spin f bands are shifted down by 2 eV and located around 7 eV, in a better agreement with experiment. Similarly the minority-spin f bands are pushed up and lie at around 8 eV. It is seen by comparing Figs. 7(b) and 7(d) that the bands coupled with minority-spin f orbitals are also dragged up to higher energy; this fictitious effect is due to the fact that the diagonal-only self-consistent GW scheme does not change the hybridization. Thus also for this material it is important to include the off-diagonal self-energy.

Figures 7(e) and 7(f) show the results of QPM and QSGW methods; again, the two schemes yield almost identical results. Although we have assumed fcc lattice structure instead of the experimentally observed hcp, the obtained results reproduce the main features of the previous QSGW calculation by Chantis *et al.*;[44] the position of majority-spin f (8 eV below the Fermi level) is in reasonable agreement with experiment while the minority-spin f levels are $\approx$4 eV too high compared to the BIS result. The unoccupied $4f$ states appear to be significantly broader than the LDA result and the experiment, implying that the $4f$ states in the GW calculation hybridize too much with the other states. Again, these point to the need for a more accurate theory beyond the GWA.

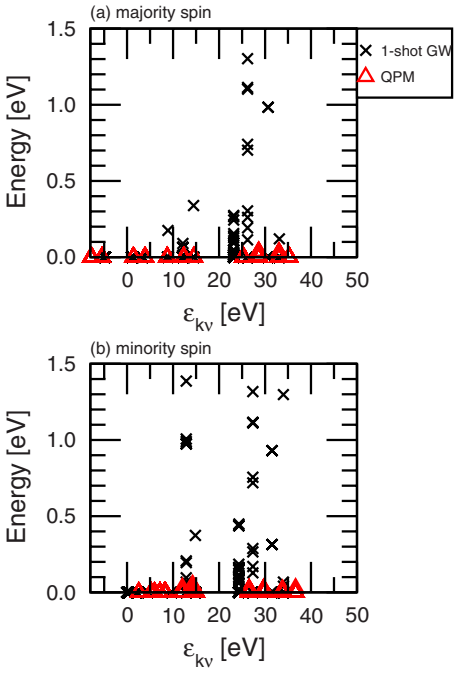

FIG. 8. (Color online) Matrix elements $|\langle\psi_{\mathbf{k}\mu}|h^{\mathrm{QSGW}}|\psi_{\mathbf{k}\nu}\rangle|$ for $\mu<\nu$ at $\mathbf{k}=(0,0,0)$ as a function of $\epsilon_{\mathbf{k}\nu}$ within the 1-shot GW (crosses) and QPM (triangles) for (a) majority-spin channel and (b) minority-spin channel.

To see the effects of the off-diagonal self-energy, in Figs. 8 and 9 we plot the off-diagonal matrix elements of h^{QSGW} and the $h_0+\Re\Sigma(\mathbf{k},\omega)$ in the basis of the effective wave functions of the 1-shot GW and the QPM. As in NiO, the wave functions and energies obtained in the QPM are found to diagonalize the QSGW Hamiltonian even though some off-diagonal matrix elements of $h_0+\Re\Sigma(\mathbf{k},\omega)$ are rather large (>1 eV). Unlike the NiO case, the off-diagonal self-energy is not very smooth near the Fermi energy, especially for the minority-spin channel. Accordingly, for Gd f bands the renormalization factor Z remains rather small ($\approx$0.5) after the self-consistent calculation as can be seen from the diagonal self-energy spectra in Fig. 10. The large off-diagonal self-energy elements and small renormalization factor Z may be an indication of the importance of many-body correlation effect for minority-spin channel that is not correctly captured in the GWA.

The above calculations of NiO and Gd indicate that for these systems the quasiparticle self-consistent solutions are not too sensitive to the choice of the effective one-particle Hamiltonian (QPM or QSGW) though further comparisons for other correlated systems and possible different forms of the effective Hamiltonian are required to see if this trend is a general one. As shown above, the solutions given by these schemes are not true quasiparticle states but may be regarded as a "one-particle limit" of the quasiparticle states within the GWA.

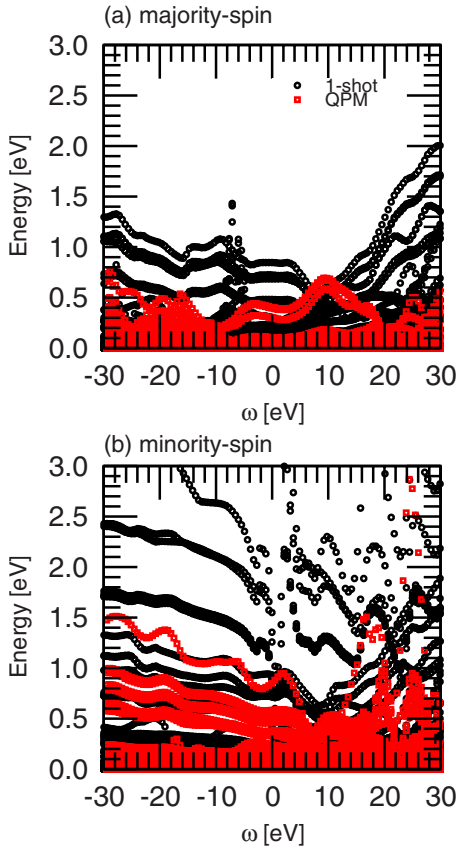

FIG. 9. (Color online) Off-diagonal elements of the Hartree Hamiltonian plus the self-energy $|\langle\psi_{\mathbf{k}\mu}|h_0+\Re\Sigma(\mathbf{k},\omega)|\psi_{\mathbf{k}\nu}\rangle|$ of Gd at $\mathbf{k}=(0,0,0)$ in 1-shot GW (circles) and QPM (squares) for (a) majority-spin channel and (b) minority-spin channel.

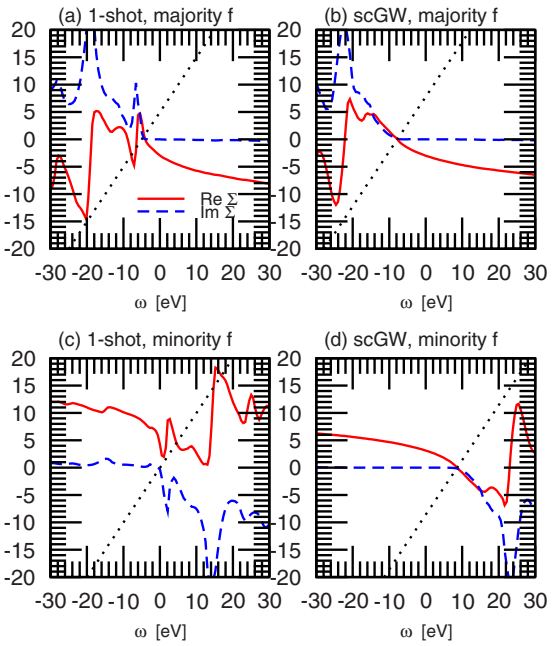

FIG. 10. (Color online) [(a) and (b)] Diagonal self-energy of majority-spin f band and [(c) and (d)] minority-spin f band at $\mathbf{k}=(0,0,0)$, obtained with [(a) and c)] 1-shot GW and [(b) and (d)] QPM. Solid lines: $\mathrm{Re}\langle\psi_{\mathbf{k}\nu}|\Delta\Sigma(\mathbf{k},\omega)|\psi_{\mathbf{k}\nu}\rangle$. Dashed lines: $\mathrm{Im}\langle\psi_{\mathbf{k}\nu}|\Delta\Sigma(\mathbf{k},\omega)|\psi_{\mathbf{k}\nu}\rangle$. Dotted lines: $\omega-\epsilon_{\mathbf{k}\nu}$.

The current results also suggest that for a given system there exists a static Hermitian Hamiltonian which reproduces the GW quasiparticle energies and the Löwdin's orthonormalized quasiparticle wave functions. The existence of a one-particle Hamiltonian with the same eigenvalues and wave functions as the true quasiparticle energies and orthonormalized quasiparticle wave functions provides a motivation for simplifying the (self-consistent) GW calculation without introducing the frequency dependence of the self-energy since self-consistent GW schemes are extremely time consuming. This may also lend some justification to static methods such as the LDA+U scheme and the recently introduced LDA+Gutzwiller method,[45] in which time-consuming direct calculations of the energy-dependent self-energy are circumvented. Evidently, the neglect of the energy dependence of the self-energy inevitably imposes some limitations. For example, it is not possible to obtain the one-particle spectral functions observed in photoemission experiments. Nevertheless the one-particle picture is sufficient in many cases for interpreting a wide range of physical phenomena.

IV. CONCLUSIONS

In this paper we have proposed a scheme, based on Löwdin's method of symmetric orthogonalization, to construct an effective one-particle Hamiltonian whose eigenenergies are the same as the quasiparticle energies and whose orthonormal eigenfunctions are the closest to the original nonorthogonal quasiparticle wave functions in the least-square sense. This procedure uniquely defines the one-particle Hamiltonian and takes into account the full frequency dependence and the off-diagonal elements of the self-energy without ambiguity.

As test cases we have applied the scheme to antiferromagnetic NiO and ferromagnetic Gd. The calculated quasiparticle energies and wave functions are found to be very close to those in the QSGW method. Our results support the idea that these schemes may be viewed as a method that gives the "best" effective mean-field solution within RPA, which may be used as a sensible starting point for calculations including higher-order many-body correlation effects.

ACKNOWLEDGMENTS

We thank J. M. Tomczak and S. Biermann for fruitful discussions. We also acknowledge the use of the full-potential LMTO-GW code provided to us by T. Kotani and M. van Schilfgaarde. The calculations were done in AIST super cluster system, Tsukuba, Japan. This work was supported by Grant-in-Aid for Scientific Research (Grant No. 19019013) and Next Generation Supercomputing Project, Nanoscience Program, and the Global Center-of-Excellence program (G-03) of MEXT Japan.

*reis@faculty.chiba-u.jp

[1] L. Hedin, Phys. Rev. **139**, A796 (1965).
[2] M. S. Hybertsen and S. G. Louie, Phys. Rev. Lett. **55**, 1418 (1985).
[3] M. S. Hybertsen and S. G. Louie, Phys. Rev. B **34**, 5390 (1986).
[4] R. W. Godby, M. Schlüter, and L. J. Sham, Phys. Rev. B **37**, 10159 (1988).
[5] F. Aryasetiawan and O. Gunnarsson, Rep. Prog. Phys. **61**, 237 (1998).
[6] W. G. Aulbur, L. Jönsson, and J. W. Wilkins, Solid State Phys. **54**, 1 (2000).
[7] G. Onida, L. Reining, and A. Rubio, Rev. Mod. Phys. **74**, 601 (2002).
[8] S. Biermann, F. Aryasetiawan, and A. Georges, Phys. Rev. Lett. **90**, 086402 (2003).
[9] F. Bruneval, F. Sottile, V. Olevano, R. Del Sole, and L. Reining, Phys. Rev. Lett. **94**, 186402 (2005).
[10] M. Shishkin, M. Marsman, and G. Kresse, Phys. Rev. Lett. **99**, 246403 (2007).
[11] B. Holm and U. von Barth, Phys. Rev. B **57**, 2108 (1998).
[12] W. Ku and A. G. Eguiluz, Phys. Rev. Lett. **89**, 126401 (2002).
[13] K. Delaney, P. Garcia-Gonzalez, A. Rubio, P. Rinke, and R. W. Godby, Phys. Rev. Lett. **93**, 249701 (2004).
[14] W. Ku and A. G. Eguiluz, Phys. Rev. Lett. **93**, 249702 (2004).
[15] P. Rinke, A. Qteish, J. Neugebauer, C. Freysoldt, and M. Scheffler, New J. Phys. **7**, 126 (2005).
[16] T. Miyake, P. Zhang, M. L. Cohen, and S. G. Louie, Phys. Rev. B **74**, 245213 (2006).
[17] E. Kioupakis, P. Zhang, M. L. Cohen, and S. G. Louie, Phys. Rev. B **77**, 155114 (2008).
[18] S. Kobayashi, Y. Nohara, S. Yamamoto, and T. Fujiwara, Phys. Rev. B **78**, 155112 (2008).
[19] F. Aryasetiawan and T. Miyake, J. Comput. Theor. Nanosci. (unpublished).
[20] S. V. Faleev, M. van Schilfgaarde, and T. Kotani, Phys. Rev. Lett. **93**, 126406 (2004).
[21] M. van Schilfgaarde, T. Kotani, and S. Faleev, Phys. Rev. Lett. **96**, 226402 (2006).
[22] T. Kotani, M. van Schilfgaarde, and S. V. Faleev, Phys. Rev. B **76**, 165106 (2007).
[23] A. Continenza, S. Massidda, and M. Posternak, Phys. Rev. B **60**, 15699 (1999).
[24] F. Aryasetiawan and O. Gunnarsson, Phys. Rev. Lett. **74**, 3221 (1995).
[25] F. Bruneval, N. Vast, and L. Reining, Phys. Rev. B **74**, 045102 (2006).
[26] P.-O. Löwdin, J. Chem. Phys. **18**, 365 (1950).
[27] R. Sakuma, T. Miyake, and F. Aryasetiawan, Phys. Rev. B **78**, 075106 (2008).
[28] B. C. Carlson and J. M. Keller, Phys. Rev. **105**, 102 (1957); for a simpler proof see also I. Mayer, Int. J. Quantum Chem. **90**, 63 (2002).
[29] J.-L. Li, G.-M. Rignanese, E. K. Chang, X. Blase, and S. G. Louie, Phys. Rev. B **66**, 035102 (2002).
[30] M. Methfessel, M. van Schilfgaarde, and R. A. Casali, *Electronic Structure and Physical Properties of Solids: The Uses of the LMTO Method*, in Lecture Notes in Physics, edited by H. Dreysse (Springer-Verlag, Berlin, 2000), Vol. 535.
[31] N. Marzari and D. Vanderbilt, Phys. Rev. B **56**, 12847 (1997).
[32] I. Souza, N. Marzari, and D. Vanderbilt, Phys. Rev. B **65**, 035109 (2001).
[33] D. R. Hamann and D. Vanderbilt, Phys. Rev. B **79**, 045109 (2009).
[34] A. A. Mostofi, J. R. Yates, Y.-S. Lee, I. Souza, D. Vanderbilt, and N. Marzari, Comput. Phys. Commun. **178**, 685 (2008).
[35] In this work we have used the LDA Kohn-Sham wave functions as a basis set; therefore we have not used the interpolation scheme suggested in Ref. 22 because the scheme requires linear muffin-tin orbitals as a basis set.
[36] Z.-X. Shen, R. S. List, D. S. Dessau, B. O. Wells, O. Jepsen, A. J. Arko, R. Barttlet, C. K. Shih, F. Parmigiani, J. C. Huang, and P. A. P. Lindberg, Phys. Rev. B **44**, 3604 (1991).
[37] G. A. Sawatzky and J. W. Allen, Phys. Rev. Lett. **53**, 2339 (1984).
[38] K. Terakura, T. Oguchi, A. R. Williams, and J. Kübler, Phys. Rev. B **30**, 4734 (1984).
[39] We note that the charge redistribution is also important in calculating the quasiparticle energy levels; if we perform self-consistent calculation without updating the charge density (Hartree potential), the position of the unoccupied e_g bands become about 2 eV higher.
[40] J. K. Lang, Y. Baer, and P. A. Cox, J. Phys. F: Met. Phys. **11**, 121 (1981).
[41] M. Heinemann and W. M. Temmerman, Phys. Rev. B **49**, 4348 (1994).
[42] V. I. Anisimov, J. Zaanen, and O. K. Andersen, Phys. Rev. B **44**, 943 (1991).
[43] B. N. Harmon, V. P. Antropov, A. I. Lichtenstein, I. V. Solovyev, and V. I. Anisimov, J. Phys. Chem. Solids **56**, 1521 (1995).
[44] A. N. Chantis, M. van Schilfgaarde, and T. Kotani, Phys. Rev. B **76**, 165126 (2007).
[45] X. Y. Deng, X. Dai, and Z. Fang, EPL **83**, 37008 (2008).